OptimalSlope: a software determining optimal pitwall shapes of maximum Overall Slope Angles leading to increased financial returns and reduced mining carbon footprint

Categoria: Investigacion y Tecnologia Minera; Operaciones Mineras

Stefano Utili[1,2]*, Andrea Agosti[1,2], Nelson Morales[3], Cristobal Valderrama[4], Robert Pell[5], Guillermo Albornoz[6]

1. OptimalSlope Ltd, London, United Kingdom

2. School of Engineering, Newcastle University, Newcastle upon Tyne, United Kingdom

3. Universite Polytechnique, Montreal, Canada

4. Itasca Chile, Santiago, Chile

5. Minviro, London, UK

6 SRK Consulting, Santiago, Chile

Abstract

The overall slope angle (OSA) of pit walls plays a crucial role in the financial return of open pit mines. The work showcases a novel design methodology where non-planar geotechnically optimal pit walls with an OSA steeper than what is used in current design practices are employed without compromising mine safety, i.e. the optimal profiles are featured by the same Factor of Safety (FoS) than their traditional design counterparts.

In the current design practice, pit wall profiles are often designed to be planar in cross-section and the profile in between ramps especially tend to be defined by a constant inter-ramp angle. Sometimes rock layers exhibiting different strengths require the inclination of a pitwall to vary with depth, but the inclination across each layer is usually constant. In this work, a new slope design software, OptimalSlope, is employed to determine geotechnically optimal pitwall profiles of depth varying inclination for the design of each sector of a copper mine located in South America. OptimalSlope seeks the solution of a mathematical optimisation problem where the overall steepness of the pitwall, from crest to toe, is maximised for an assigned lithology, rock properties, and FoS. Bench geometries (bench height, face inclination, minimum berm width) are imposed in the optimisation as constraints that bind the maximum local inclination of the sought optimal profile, together with any other constraints such as geological discontinuities that may influence slope failure. The obtained optimal profiles are always steeper than their planar counterparts up to 8° depending on rock type and severity of constraints on local inclinations. The adoption of overall steeper profiles leads to a reduction in the amount of waste rock and, consequently, the stripping ratio.

To quantify the improvement obtained by adopting geotechnically optimal profiles, we performed two designs: one employing planar pit walls and another one adopting the optimal pitwall profiles determined by OptimalSlope. In determining the Ultimate Pit Limit (UPL) and pushbacks, we sought to maximise the net present value (NPV) and achieve an annual production schedule as uniform as possible over the mine lifetime. The FoS adopted for both planar and optimal pitwall is the same, with verifications performed by limit equilibrium (LE) method analyses (Morgenstein–Price method) run in Rocscience Slide2 and finite difference method analyses with strength reduction technique run in FLAC3D on the 2D UPL sections. Also, a 3D stability analysis of the entire UPL was performed in FLAC3D. For each mine, we assess both financial gains (in terms of NPV) and environmental gains (measuring the reduction in carbon footprint and energy consumption).

Keywords: strategic open pit mine design; optimal pitwalls; NPV optimization; rockwaste reduction;

carbon footprint reduction; OptimalSlope

Introduction

In the last four decades a clear trend of open pit mines being excavated at increasing depths is apparent (Figure 1a). As existing mines deepen owing to the increased efficiency of mining equipment and improved exploration techniques and technology, the ore bodies left to be exploited are everywhere deeper (Figure 1b). Between 1930 and 2000, the depth of the average discovery in Australia, Canada, and the United States increased from surface outcropping to 295 m [1]. As a consequence, ensuring pitwalls as steep as possible has grown in importance since the deeper a mine, the higher the effect of pitwall steepness on the amount of rockwaste to be excavated and therefore mine profitability [2].

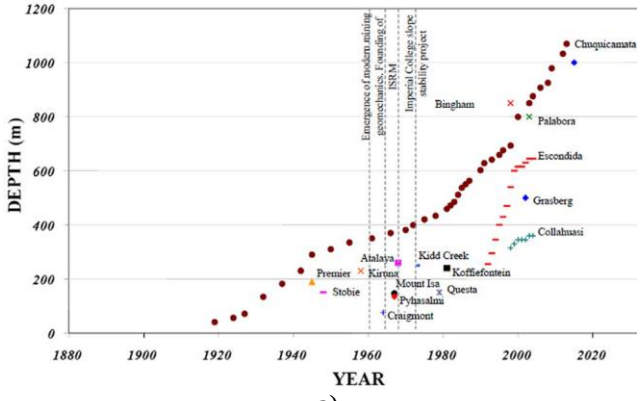

a)

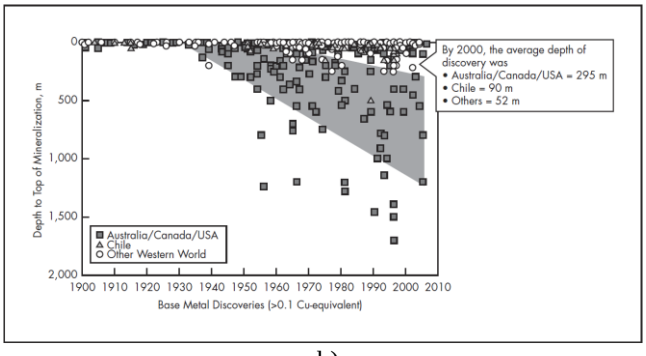

b)

Figure 1. a) Increasing depth of open pit mines over the years, after [3]; b) average depth of newly discovered ore deposits, after [1].

Also, there is an increasing trend to excavate pits of significant depth in weak rocks such as saprolites [4]. In weak rocks the steepness of the pitwalls is lower than the one for pits excavated in competent rock to prevent slope failures. This in turn implies more waste rock is produced. Therefore, any gain in the overall slope angle (OSA) of pitwalls is more important than ever for the economic profitability of open pit mines.

Anecdotal evidence of the fact that a slope profile non-linear in cross-section, i.e. a profile whose inclination varies with depth, is better than a linear one, i.e. a planar profile, was reported as far back as 1890 [5]. In fact, Newman [5] observed that cuttings of concave shape excavated in homogeneous clay layers tended to be more stable than planar ones with the same OSA which in turn are more stable than cuttings of convex shape (Figure 2a). Many decades later, Hoek & Bray in chapter 12 of the second edition of *Rock slope engineering* [6] analyze the stability of some concave circular slopes in cross-section. Assuming the slopes to be excavated in homogeneous rock and using the Mohr-Coulomb (M-C) failure criterion to characterize its strength, i.e. cohesion, c, and internal friction angle, φ, they found a higher stability number (which is a dimensionless index capturing the mechanical stability of a slope that will be introduced in "Methodology") for circular profiles than for their planar counterparts, *i.e.* the planar slopes with the same OSA which share the same toe and crest points. They also mention that circular shapes had been considered by [7] for the design of the pitwalls of an iron pit mine in Canada. However, Hoek & Bray strongly caution against the assumption of uniform slope since it completely disregards the fact that the strength of geomaterials tends to vary with depth, being usually lower in the upper part of the excavated slope due to well-known geological processes (e.g. soil deposition, weathering, etc.). The first systematic theoretical study on the mechanical properties of concave slope profiles for geomaterials exhibiting some cohesion, so applicable to all rocks and clayey soils, appeared in [8]. In that study, the superior stability of logarithmic spiral (logspiral) profiles, with the logspiral being featured by a radius of curvature increasing with the depth of excavation (Figure 2b), was systematically proven over their planar counterparts having assumed the slopes to be uniform and with strength characterized by c and f. By employing the limit analysis upper bound method, Utili & Nova [8] first systematically determined the optimal logspiral shape, *i.e.* the shape associated to the highest stability number for several prescribed OSAs, second compared the optimal logspiral slopes to their planar counterparts. They show that logspiral profiles exhibit higher FoS than their planar counterparts for any value of *c*, and φ considered with

the highest gain for inclinations midway φ and the vertical line, *i.e.* for $\mathrm{OSA}\sim\frac{\pi}{4}+\frac{\varphi}{2}$. Since then, other researchers ([9-11]) have independently investigated the stability of concave profiles excavated in a uniform $c-\varphi$ geomaterial, employing different methods, namely the slip line method [9], limit equilibrium methods [10] and the finite element method for the assessment of slope stability. They all reached the same conclusion concerning the superior stability of non-linear concave profiles. However, a key limitation of these studies is the assumption of a specific shape, either a circle [10] or a log-spiral [8] or a curve stemming from the slip-line field theory and the associated characteristic equations [9], so that the shape claimed to be optimal is found as the shape associated to the highest stability number among curves belonging to a very restricted family. It is obvious that these profiles are instead sub-optimal and the shape of the truly optimal profile cannot be inferred from the aforementioned studies. In fact in the case of a profile to be excavated in a uniform c - φ geomaterial, the optimal shape calculated by OptimalSlope [12] turns out to be partly concave and partly convex (see figure 2c) so significantly different from the purely concave shapes considered in [8-11]. Another perhaps even more important limitation resides in the assumption of uniform slope present in all the aforementioned methods that prevents the application of these findings to real open pit mines which are typically featured by complex lithologies involving multiple rock formations of different mechanical strengths and various geological discontinuities.

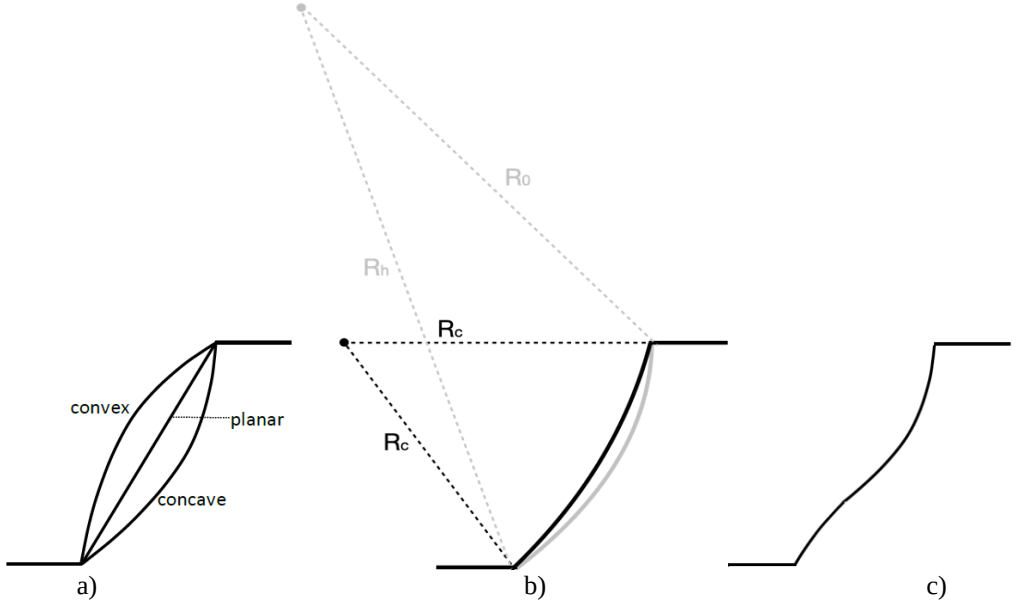

Figure 2. Slopes of different shapes: a) a concave, planar and convex slope profile with the same overall slope angle; b) profiles excavated into a uniform c, ϕ slope: logspiral optimal profile (gray line) redrawn after [8] and circular optimal profile (black line) redrawn after [10]. Since a circle is a particular case of a logspiral, *i.e.* a logspiral with a constant radius (rather than variable), an optimal logspiral profile is always more stable than an optimal circular one. c) optimal profile partly concave and partly convex obtained by OptimalSlope for a uniform c, ϕ slope.

The search for the optimal shape of a slope profile is a difficult problem of topological optimization since slopes develop very significant irrecoverable (plastic) deformations which cause significant stress redistribution to occur before reaching failure, but the theory of topological optimization developed so far in engineering deals predominantly with elastic media [13]. Neglecting the onset of plastic deformations in a slope, *i.e.* assuming a purely elastic behavior, is not a viable option since this would severely underestimate the slope resistance to failure hence the slope Factor of Safety. And the application of plasticity theory to topological optimization is only in its infancy [14]. Therefore current algorithms in the literature for topological optimization are not viable to search for the optimal profile of slopes. The code OptimalSlope exploits the fact that slope failures occur either as a rotational mechanism (a planar failure being a particular type of rotational failure with an infinite radius of curvature) or mechanisms whose kinematics

is dictated by the presence of discontinuities (e.g. the interface between two rock layers, a fault, joints, beddings etc.). For a homogeneous slope in a c - φ geomaterial, the limit analysis upper bound method allows to find the critical rotational mechanism simply by determining the minimum of an analytical objective function without requiring any discretization of the slope into finite elements [15]. The function is obtained imposing the energy balance between the external work done by the mass of the candidate failure mechanism and the energy dissipated along its failure surface. The equation has been extended to find the critical mechanism for piecewise linear slope profiles in a uniform layer and then to the case of layered slopes [12]. Also, the formulation has been extended to slopes in rocks obeying the generalized Hoek-Brown (G-H-B) failure criterion [16,17]. The minimum of the function stemming from the energy balance equation and therefore the critical mechanism is found by OptimalSlope [12]. Since the time the G-H-B criterion was introduced, a strong consensus has gathered in the rock mechanics community that it is a better criterion than M-C to describe the strength of rock masses [18,19]. But for highly weathered rocks and residual soils M-C is better [4], so there are several cases of mines where the M-C criterion is employed to fit the rock strength data of some layers whilst the G-H-B criterion for some other layers. OptimalSlope can deal with these situations too, i.e. some rock layers being characterized by the M-C criterion whilst others by the G-H-B criterion, since the G-H-B parameters of any layer are converted by OptimalSlope into equivalent c - φ parameters, employing the method of Renani & Martin [20].

In the excavation of an open pit, several rock layers of different strength are usually encountered. OptimalSlope can find the optimal profile for any specified lithological sequence (any number of layers can be specified as input with each layer strength characterized by either M-C or G-H-B parameters) without unduly restricting the search to any predefined family of shapes. The optimal slope profile is found as the solution of a mathematical optimization problem where the OSA of the slope, i.e. the inclination from slope crest to toe, is maximized for an assigned stratigraphy, rock strength properties and a prescribed FoS. Geometric requirements stemming from bench sizes (bench height, face inclination and minimum berm width) are imposed as constraints binding the maximum local inclination of the sought optimal profile together with any other geometric constraint, e.g. constraints to prevent the occurrence of local failure mechanisms due to geological discontinuities such as faults and joints (see "Methodology").

In the next section of the paper, the case study considered to demonstrate the financial and environmental benefits stemming from the adoption of optimal profiles for mine pitwalls is described. Then in "Methodology" the methodology employed is provided followed by results in "Results" and conclusions. In the Methodology section it will be illustrated how the proprietary code OptimalSlope [21] works and interacts with the mining software packages employed to perform strategic pit design.

Case study

The block model of the copper deposit employed as case study has been provided by a mining company collaborating with the Delphos Mine Planning Laboratory at the University of Chile (Figure 3). Due to a Non-Disclosure Agreement (NDA), its name and location cannot be revealed. All the parameters needed to perform the pit design were taken from [22] except for the Mining Cost Adjustment Factor (MCAF), which was estimated for this study. The characteristics of the block model are as follows: cubic blocks of 10 m x 10 m x 10 m, block model dimensions of 2250 m x 2250 m x 360 m, 647446 blocks in total. From the site lithology and geotechnical properties, two roughly uniform pit sectors were identified in [22] (see Figure 4). In each pit sector, one representative cross-section was assumed to design the pitwall profile.

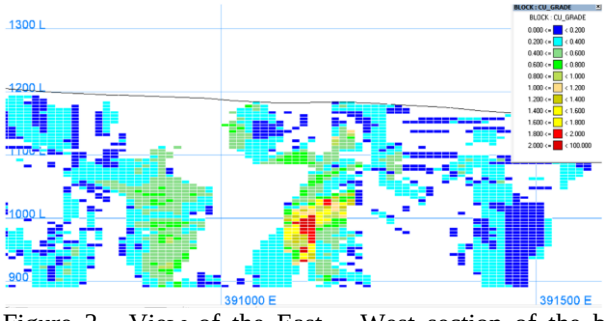

Figure 3. View of the East – West section of the block model (after [22]).

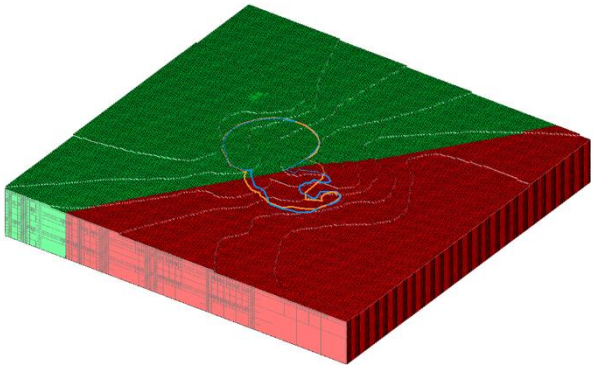

Figure 4. 3D view of the block model and the pit sectors: in red are the blocks in sector 1 and in green the blocks in sector 2. In the middle of the topographic surface the boundary of the Ultimate Pit Limit (UPL) is visible: the orange curve for the UPL obtained in case of planar pitwalls and the blue curve for the UPL obtained in case of optimal pitwalls.

The rock geotechnical parameters are reported in table 1. The rock strength is characterized by the G-H-B failure criterion [16]. The uniaxial compression strength (UCS), the Geological Strength Index (GSI), mi and the disturbance factor (D) are all provided in the table. The disturbance factor is to account for rock weakening due to blasting and stress relaxation. We acknowledge that assuming D=1 throughout the rock mass is overly conservative since in modern mines blasting is well controlled. Also, the depth of the open pit is such that the amount of stress relaxation is unlikely to cause significant damage. However, we opted to retain the assumption of D=1 to be consistent with the set of input data from [22], thus accepting a significant degree of conservativism on the value of this parameter.

Table 1. Geotechnical properties after [22]

	UCS [MPa]	GSI [-]	mi [-]	D [-]	γ [kN/m^3]
sector S1	65	45	15	1	25.9
sector S2	50	45	12	1	25.9

The values adopted for the economic parameters and metallurgical recovery together with the discount rate assumed were taken from [22] and are listed in Table 2. With regard to the capital costs, in [22] only the cost for the processing plant is accounted for. Here instead, we wanted to account for all the typical costs needed in an open pit mine project: they are provided in Table 3.

Table 2. Economic parameters and metallurgical recovery taken from [22]

Copper price	[USD/t] 6000	[USD/lb] 3
Selling cost	[USD/t] 1700	[USD/lb] 0.85
Reference mining cost [USD/t]	3.4	
Processing cost [USD/t]	6.1	
Metallurgical recovery [%]	85	
MCAF [USD/t/bench]	0.13	
Discount rate (%)	10	
Processing method limit [mtpy]	5	
Mining limit [mtpy]	10	

Table 3. Breakdown of the capital costs considered

AREA	DESCRIPTION	COST [million USD]
Mining	Mine infrastructure	11.2
Processing plant	Concentrate thickening, filtration & storage	5.7
	Grinding plant	99.0
	Flotation & regrinding plant	28.3
	Moly plant	3.7
	Subtotal	*136.7*
Crushing	Primary crushing, coarse ore handling	45.0
Tailing	Tailings thickening & water recovery	9.5
Infrastructures	Plant infrastructure	9.6
Ancillaries	Services	34.5
	General area	3.4
	Subtotal	*37.9*
TOTAL DIRECT COSTS		**250.0**

Methodology

The design of pitwalls in open pit mines is an iterative process involving a multidisciplinary team of geologists, geotechnical engineers and mining engineers [1]. The design process requires iterative steps between the teams [23]. Typically, several boreholes are drilled as part of a site investigation and laboratory tests are performed on the core samples retrieved to characterize the mechanical strength of the geomaterials encountered and the key lithological units. Then, a preliminary simplified design is performed and a pit crest contour is drawn. The pit is then split into sectors in order to design the pitwalls [23]. It is wise to divide the mine in sectors small enough so that a 2D vertical cross-section representative of the lithology of the sector can be determined for each sector. Then for each sector cross-section a pitwall profile needs to be designed as steep as possible and at the same time to satisfy a

prescribed FoS against slope failure. The pitwall profiles are then prescribed as input together with the relevant economic and metallurgical data for the mine into a pit optimizer software package to calculate the optimal Ultimate Pit Limit and pushbacks. These are typically based on the Lerch-Grossman algorithm [24] or the more recent pseudo-flow [25]. Both algorithms require to identify precedences between blocks of the block model lying within the pit boundary. How block precedences are built for pitwalls with depth varying inclinations is well described in [26,27].

The iterative procedure we followed to calculate the UPL is illustrated in Figure 5. The procedure is the same irrespective of the shape of the pitwall profile adopted, *i.e.* planar or optimal profile: at the beginning, an initial pit depth (H_0) was assumed as equal to the total height of the block model minus the air blocks so $H_{UP\,L\,S1,0} = H_{UP\,L\,S2,0} = 370$ m with $H_{UP\,L\,S1,0}$ and $H_{UP\,L\,S2,0}$ indicating the pitwall height in sector S1 and S2 respectively. Then, we calculated the representative pitwall profiles for the specified pit depth in each sector: in case of planar pitwalls employing Limit Equilibrium Method (LEM) analyses by Slide 2 [28] whereas for optimal pitwalls employing OptimalSlope (see "Pitwall design"). Then we assigned the pitwall profiles into the pit optimizer (Geovia Whittle 4.7.3) and ran it to produce the UPL (the steps entailed are described in "Pit optimization").

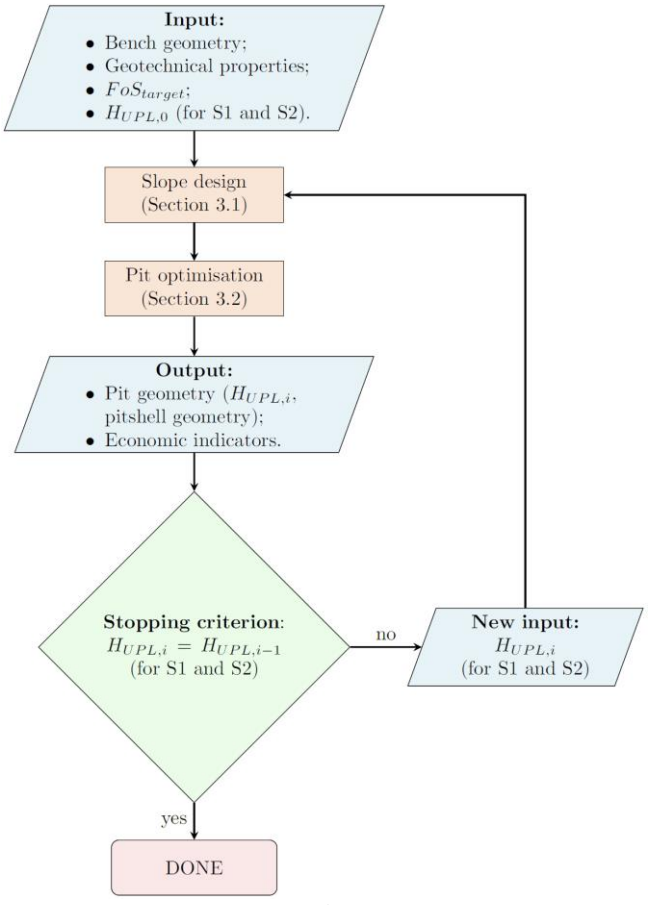

a)

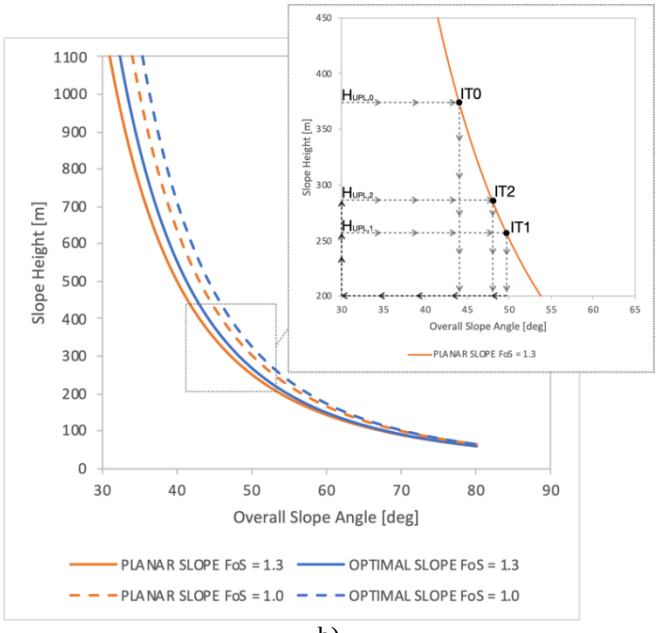

b)

Figure 5. Pit design process: a) flow chart illustrating the iterative process followed to determine the Ultimate Pit Limit (UPL) and pushbacks. Note that the process is the same irrespective of the shape of the adopted pitwall profiles. b) Slope (pitwall) height versus Overall Slope Angle (OSA) for different FoS values and profile shapes (planar profiles in orange and optimal profiles in blue). Note

the curves were derived for the specific geotechnical parameters of the case study mine. A different set of strength parameters would produce different curves, however the qualitative trend of the curves is valid irrespective of the rock strength values. In the inset a graphical representation of the iterations performed to arrive at the OSA for each pit sector is provided: the gray arrows refer to the slope design process that produces pitwall profiles from an assigned height (section "Pitwall design"), the black arrows refer to the pit optimisation process that produces the UPL depth from assigned pitwall profiles (section "Pit optimization").

The detail of the procedure followed to integrate OptimalSlope with Geovia is presented in Figure 6. In the figure it is also illustrated how to integrate OptimalSlope with three other major commercial mining software packages, namely Datamine, Maptek and Hexagon Mining. Note that conceptually the process is independent of the software package employed, but the names of the software modules to manipulate the block model, their scripting languages and some routines within the pit optimizers may differ. For this reason we verified that the design procedure here employed was applicable in all the software packages mentioned in Figure 6, namely Geovia Surpac [29] and Whittle [30], Datamine Studio OP [31] and Studio NPVS [32], Maptek Vulcan Open Pit Mine Planning [33] and Hexagon MinePlan3D [34] and Project evaluator [35], to ensure the pit optimization procedure herein described works correctly with each software package.

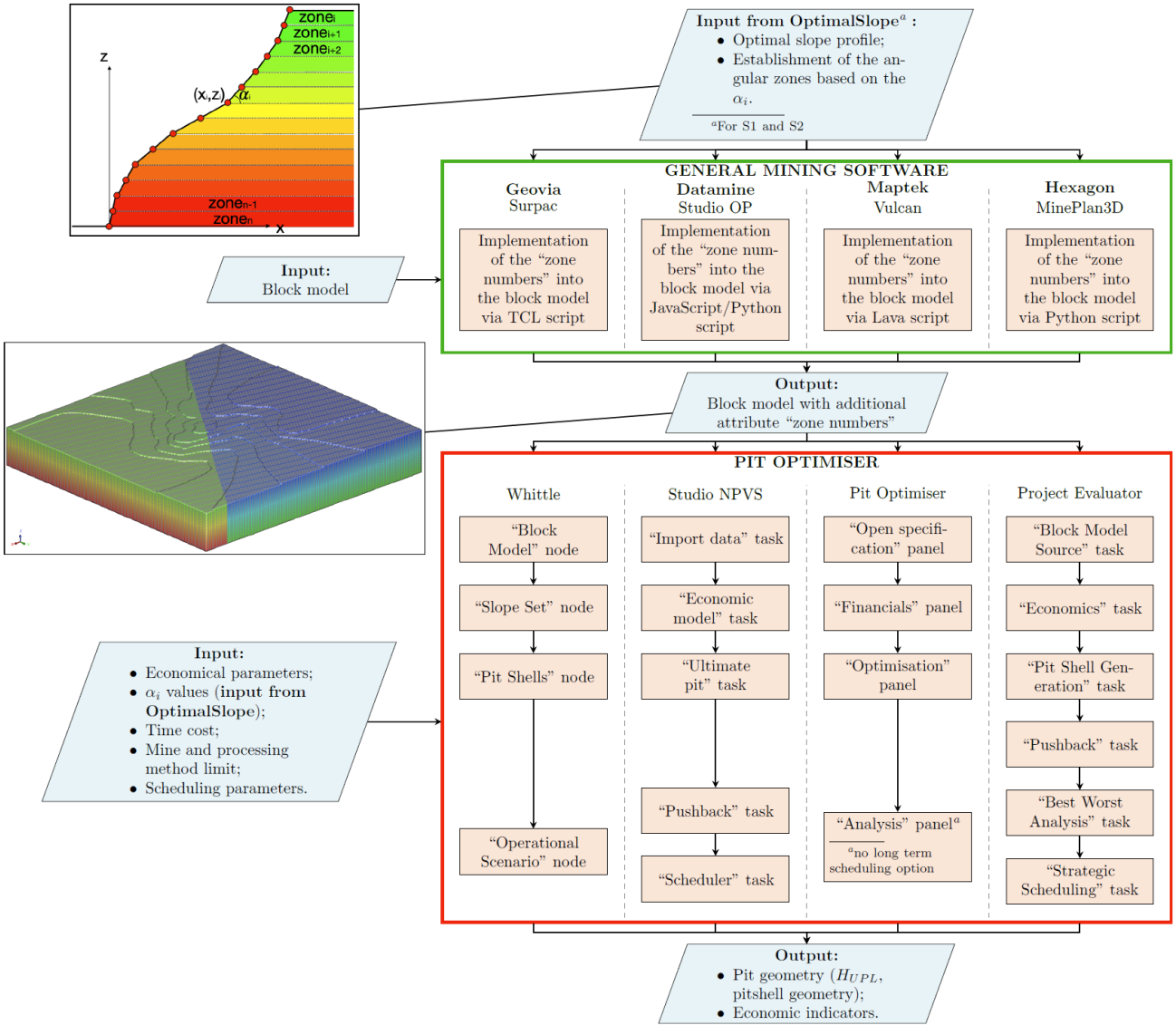

Figure 6. Flow chart illustrating how OptimalSlope [21]interacts with major commercial mining software packages, namely Geovia, Datamine, Maptek and Hexagon Mining to perform a pit design. Going from top to bottom: 1) OptimalSlope produces the optimal slope profile for the UPL of each sector of the pit; 2) the profiles are prescribed for each pit sector in the block model in the standard way by specifying an inclination ai for the row(s) of blocks lying within each segment of the profile of constant inclination (note that there is more than a way slopes can be specified, we chose to do it by an additional block model attribute and grouping blocks in zones since for all the blocks exhibiting the same inclination, so belonging to the same zone, the angle can be assigned with one instruction only); 3) the pit optimizer is run as usual to determine the UPL and pushbacks. In the PIT OPTIMIZER red box we report the names of the nodes / tasks / panels used to specified the input data and run the pit optimization.

The UPL depths obtained as output of the strategic pit optimization, $H_{UP\ L\ S1,1}$ for sector S1 and $H_{UP\ L\ S2,1}$ for sector S2 were then compared to the values prescribed as input in the slope design process, $H_{UP\ L\ S1,0}$ and $H_{UP\ L\ S2,0}$, respectively. Since they turned out to be different, a second iteration was performed where $H_{UP\ L\ S1,1}$ and $H_{UP\ L\ S2,1}$ were assumed as input for a second slope design process followed by a second run of the pit optimizer. The iterations were then stopped when the UPL depths obtained as output of the pit optimizer ended up being equal to the values prescribed as input in the slope design process for each pit sector. The iterations required to reach convergence are reported in Table 5.

Pitwall design

Open pit mines are increasingly excavated in complex lithologies where usually different failure mechanisms (e.g. bench failure, interramp failure, overall slope shear failure, failures involving faults and discontinuities etc.) turn out to be dominant in different sectors of the pit so that they all need to be analysed. In the design of pitwalls, we followed the standard practice of starting with the design of benches and then moved to the overall pitwall profiles [36,37].

To determine the maximum inclination of each face bench we performed Limit Equilibrium Method Morgenstern-Price analyses using the Rocscience program Slide 2 [28] to satisfy the prescribed Factor of Safety (in this case FoS=1.1, see Table 4). In general the amount of backbreak and the effective bench face angle are controlled by the joints and faults intersecting each bench. Here, joints were not considered purely due to the lack of this type of data for the mine analysed. If data on joints and faults were available, software packages such as SWedge [38] or Frac_Rock [39] would allow determining the maximum inclination of each face bench.

Table 4. Acceptability criteria for Factor of Safety

$FoS_{min,bench}$	1.1
$FoS_{min,UPL}$	1.3

The height of the benches adopted for the whole mine is 10m [22]. Consistently with the set of input data from [22], we computed the minimum berm width, b_w, using the equation proposed by Call [40] known as the modified Ritchie's criteria, which has been demonstrated to be effective in field tests in several benched mine slopes [41]:

$$b_w[m] = 4.5[m] + 0.2 * H_{bench} \quad (1)$$

We acknowledge that another equation, $b_w[m] = 3.5[m] + 0.17 * H_{bench}$, was proposed in [41] although having the shortcoming of being less conservative [42] so we preferred to use Eq. (1).

Berms have multiple objectives that need to be met when establishing a berm width, the most important ones being rockfall retention, capture of debris from bench excavation and operations of the chosen fleet of excavators. With regard to rockfall retention, berm widths are not designed for 100% retention of rockfalls since this would lead to unviably large widths but instead to shelter most of the rockfall. Eq. (1) leads to 70-85% retention of rockfall volumes [18]. Such a percentage may be less than what a mining company would wish for. For this reason, in the last two decades, several rock fall researches were performed utilising numerical simulations considering potential trajectories on slope designs using either two-dimensional lumped-mass impact models (2DLM), e.g. the Rocscience code RocFall [43], and/or — three-dimensional rigid body impact models (3DRB) such as the code 'Trajec3D' [44]. These numerical models use coefficients of restitution to characterise the amount of energy lost due to the inelastic deformations stemming from the collision of a rock fragment bouncing over a berm or bench. Unfortunately the input parameters are vastly different for 2DLM and 3DRB. Also they are seldom calibrated with any site-specific rock fall case studies or field test data at the mine feasibility stage, and may

remain uncalibrated throughout the operating life of the mine [45]. In conclusion, given the amount of information available at the feasibility stage of mine design, we believe Eq. (1) is adequate to establish minimum berm widths especially given the (low) bench heights of our case [45]. Finally, note that as pointed out in [18, see section 10.2.1.2], Eq. (1) is still largely used by practitioners in North and South America. Another requirement for the chosen berm width is the ability to capture most debris falling from the bench face above due to unstable wedges. The adequacy of the chosen berm widths can be verified via either computer modelling [39] or analytical equations [46]. In [47] a recent extensive review of the bench design methodologies currently employed by the open pit mine industry is provided.

After the computation of the bench geometries we computed the geotechnically optimal slope profiles for the cross-sections of the two pit sectors of the mine (Figure 4) using the proprietary code OptimalSlope [21]. The code requires bench height, bench face inclination, minimum berm width and road width as input from the user (see figure 7) since these geometric data will act as constraints in the search for the optimal profile. Any pitwall profile is defined in OptimalSlope by a discrete set of points in the vertical plane: see the (x_i, z_i) coordinates in Figure 8, with z_i being values specified according to the bench height (Dz = bench height) input by the user whilst x_i are unknown variables to be determined. The search for the optimal profile is constrained to feasible profiles (which lie within the red and blue bounds of figure 8). A profile is feasible if $\frac{z_i - z_{i-1}}{x_i - x_{i-1}} \leq \tan \alpha_{i\max}$ for every *i*, *i.e.* the inclination of each segment of the profile is capped to $\alpha_{i\max}$. The $\alpha_{i\max}$ values are determined by the code before the optimization algorithm is called on the basis of bench height, bench face inclination and minimum berm width provided by the user. In case a ramp needs to be included as part of the pitwall profile, a lower $\alpha_{i\max}$ value is imposed for the profile segment corresponding to the vertical position of the ramp.

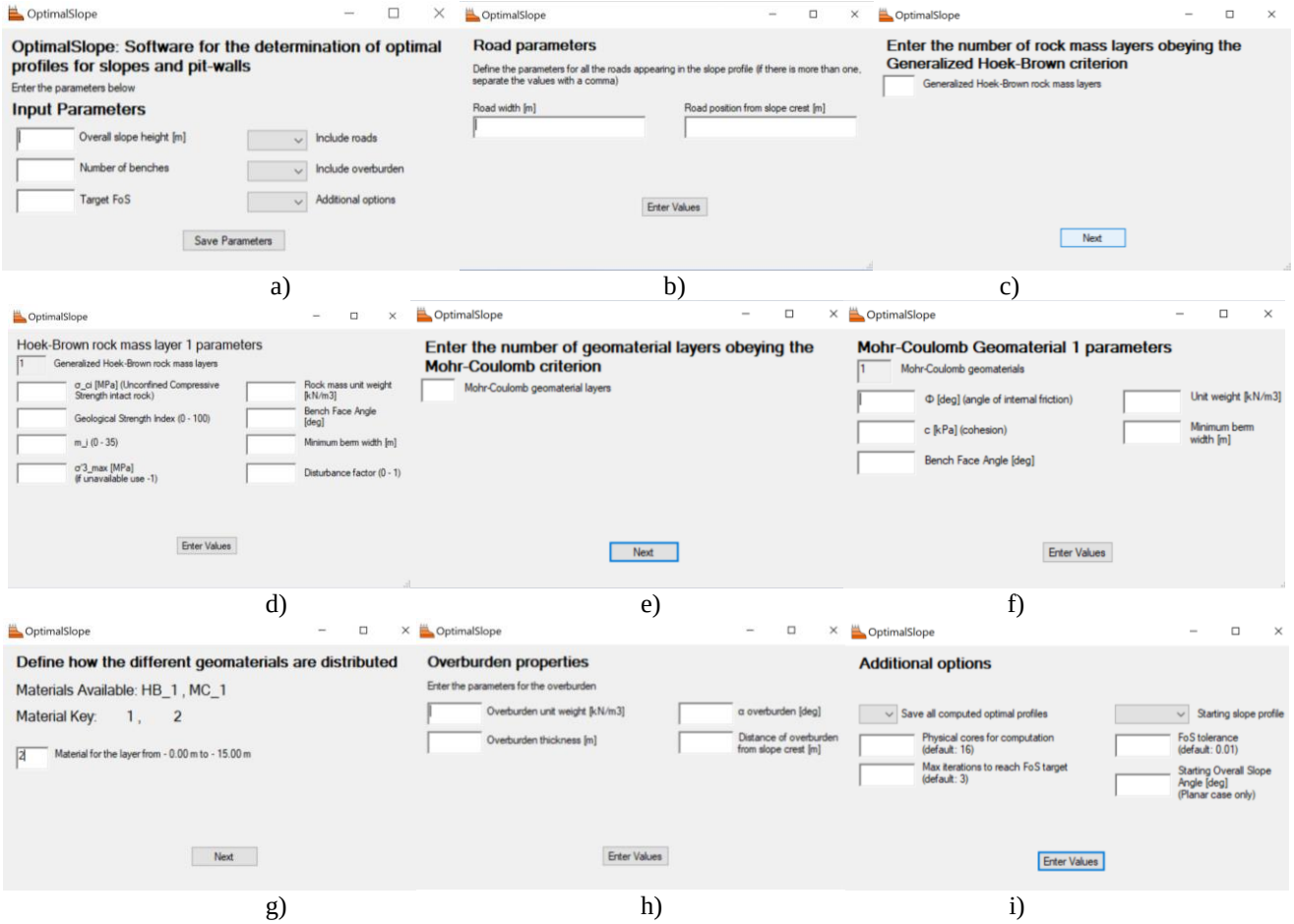

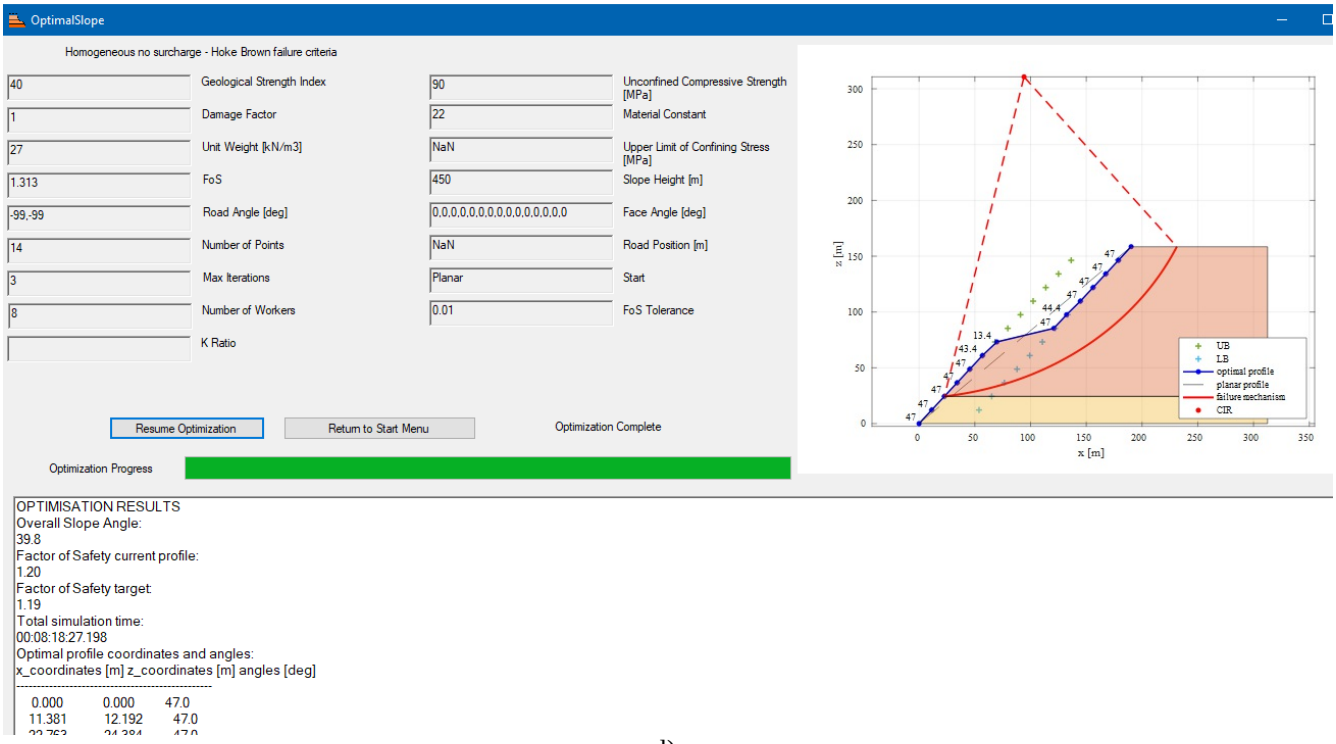

l)

Figure 1: OptimalSlope Graphical User Interface with data input (screens a; b; c; d; e; f; g; h; i) and output (screen l). Bench and ramp geometries are requested so that the optimal profile complies with all the geometric constraints stemming from bench design and presence of any ramps.

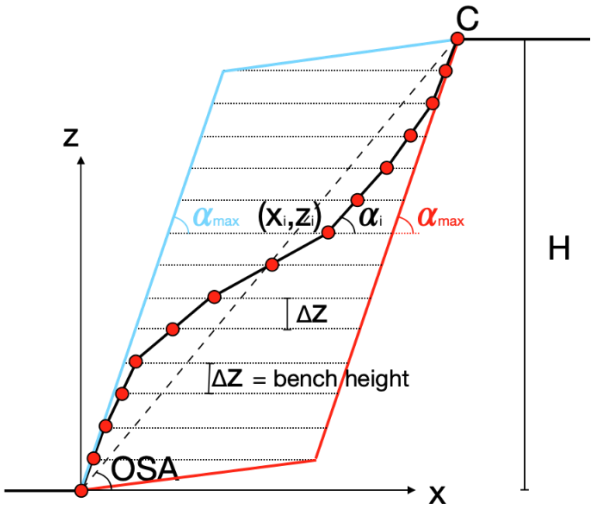

a)

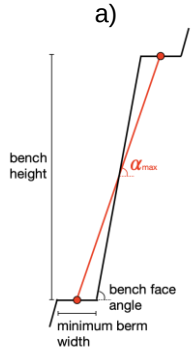

b)

Fig 8 a) A generic candidate slope profile. The toe of the profile is at the axes origin (x_0, y_0), point C is the slope crest. A uniform discretization along the z direction is adopted. The red and blue lines enclose the region where the profiles are sought. The profile is discretised in n Δz intervals so there are n-1 unknowns to be determined: x_1, x_2, …x_{n-1}. In the context of open pit mines, a good choice of Δz is to assume Δz equal to the bench height. b) Determination of $\alpha_{i\max}$ based on bench geometry (input to OptimalSlope).

The optimal pitwall profile is defined as the overall steepest safe profile, *i.e.* OSA=OSA_{max}, with OSA being the inclination over the horizontal of the line joining the pitwall toe to the crest (see Figure 8). OSA_{max} is determined by OptimalSlope iteratively (see Figure 9). The main algorithm finds the optimal pitwall shape for an assigned OSA and geometric constraints ($\alpha_{i\max}$ values). An initial guess OSA value is first determined for the specified pitwall height, the geotechnical properties of all the layers and the specified FoS on the basis of a database of stability charts based on [48] built in OptimalSlope. In case of rock strength described by G-H-B, the conversion of the H-B parameters to M-C was performed via Eq (14) in [20]. Note that a few equations for the conversion of the G-H-B parameters into M-C for rock slope stability

analyses have been proposed in the literature with [49,50] being the most prominent. All these relationships depend on the range of confining stress experienced by the slope. Hence, the main challenge in finding equivalent strength criteria is selecting the appropriate range of confinement. However contrary to what the previous relationships suggest, the appropriate range of confinement was shown in [20] to be insensitive to rock mass strength and instead primarily controlled by the slope geometry and only the equation proposed in [20] reflects such a dependency. The FoS_i associated to the optimal profile found at the *i*-th iteration is then compared to the target FoS_{target}: if it is higher a steeper OSA is prescribed at the next iteration, viceversa if lower a less steep OSA is prescribed. The termination criterion is specified in terms of the percentage difference between FoS_{target} and FoS_i. For the pitwalls of the case study considered four iterations were enough to obtain a FoS less than 1% different from FoS_{target}.

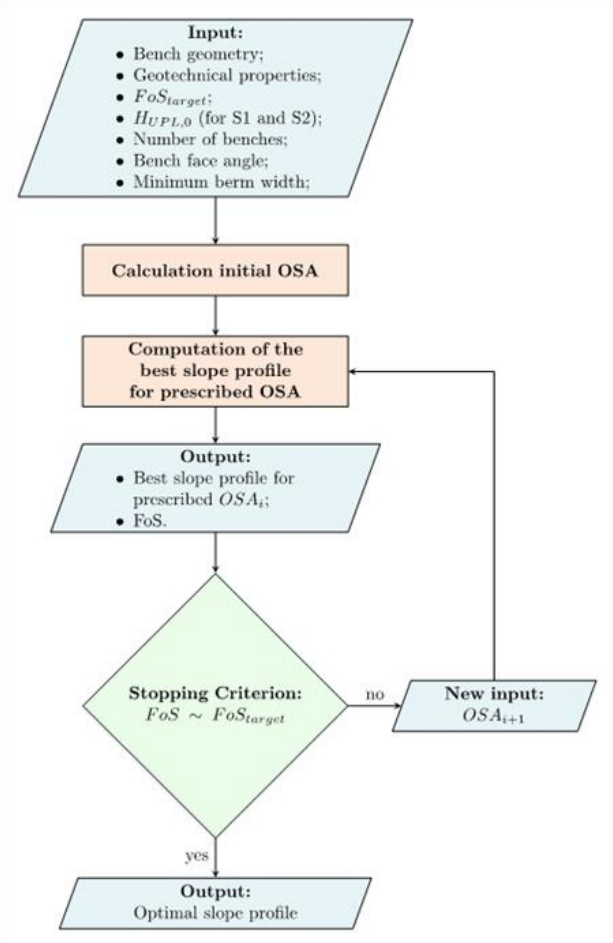

Fig 9 illustration of the iterative procedure used by OptimalSlope to determine the optimal profile for a given pitwall.

In case of a homogeneous slope, *i.e.* a single uniform rock/soil layer, the optimal profile shape is found by the main algorithm for a prescribed input OSA as the profile associated to the largest stability factor defined as $N_s = \frac{\gamma H}{c}$ in case of the M-C criterion or $N_s = \frac{\gamma H}{\sigma_{ci}}$ in case of the G-H-B criterion. N_s is a well known single scalar parameter which was introduced by Taylor [51,52] in drawing dimensionless stability charts and is the appropriate metric to compare the performance of different slope profiles [21]. In case of a layered (non-homogeneous) slope OptimalSlope determines the optimal profile as the profile associated to the maximum of an equivalent N_s which is calculated as a physically based weighted average of the γ, H, c or σ_{ci} parameters of all the slope layers. Note that in a layered slope a failure mechanism may go through several layers of vastly different strength so the length of the failure surface (a curve in 2D) in each layer may affect significantly the overall resistance (i.e. the amount of energy dissipated in the limit analysis energy balance equation). Therefore OptimalSlope calculates the energy dissipated along the failure surface of each candidate mechanism considered based on the actual length of the failure curve present in each layer ensuring the N_s calculated for each mechanism considered is a true reflection of the mechanism stability factor (see Figure 10). Crucially to determine the stability factor of any candidate profile shape, all the possible failure mechanisms are considered by OptimalSlope including any failure surface daylighting everywhere above the slope toe (see Figure 10).

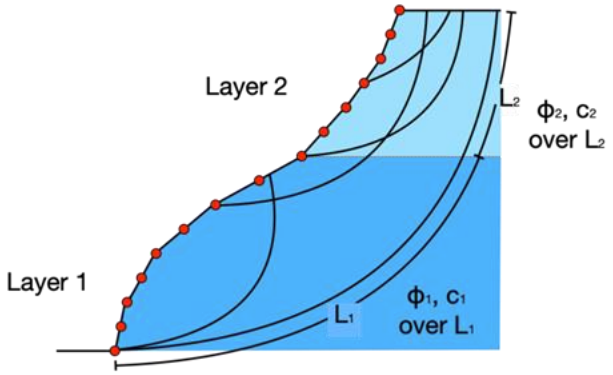

Fig 10 Illustration of the failure mechanisms considered by OptimalSlope for a generic candidate profile in a layered slope with layers of different strength.

Pit optimization

To assign the pitwall profiles into the pit optimizer

Geovia Whittle, we split the block model into 'zones' (according to the Whittle terminology) using Geovia Surpac and assigned a slope inclination to each 'zone'. The number of zones to be employed depends on the shape of the pitwall profile (see Figure 6). Then, to compute the ultimate pit limit and pushbacks, first we ran Whittle to produce the discounted best case scenario curve in the pit-by-pit graph (see Figure 15). Next we employed the so-called 'Milawa NPV' algorithm to generate a specified case scenario curve for an initial set of pushbacks, chosen in correspondence of sharp increases exhibited by the best case scenario curve. Then we recomputed the specified case scenario curve a few times exploring the choice of different pit-shells as pushbacks nearby the ones initially selected to make the specified case curve as close to the best case scenario as possible. Having found the combination of pushbacks that maximizes the NPV of the UPL, we plotted the annual ore production scheduling graph (Figure 16) and changed the selection of pushbacks if needed to ensure an annual tonnage input to the processing plant as uniform as possible over the mine lifetime. Finally, we chose the UPL in correspondence of the highest point of the plateau exhibited by the specified case curve (Figure 15). We are aware practitioners may make slightly different choices: for instance they may decide to pick a pitshell different from the one associated to the peak of the specified case scenario as UPL for various considerations (to maximize the amount of ore extracted or of reserve amount or due to operational reasons) and may not be willing to iterate for the selection of pushbacks and UPL. Moreover, design practices vary between practitioners due to different company objectives and designer experiences. Nevertheless, the key objective of the design exercise performed here is to run a consistent and meaningful comparison between the traditional design based on planar pitwalls and the one here proposed based on geotechnically optimal pitwalls in order to quantify in a rigorous way the financial and environmental gains due to the adoption of geotechnically optimal profiles. To this end it is logical to adopt the same procedure for the selection of UPL and pushbacks irrespective of the pitwall profile shapes. We also believe that even if design objectives different from the one used here were to be adopted (e.g., compromising some NPV to maximize reserve conservation) and even if the procedure for the determination of UPL and pushbacks was different from the one adopted here (e.g. prioritizing payback time over NPV maximization, using bench discounting, etc.), the adoption of optimal profiles for the pitwalls will always bring financial and environmental gains since it leads to a reduced amount of waste rock excavated whatever the design procedure and corporate priorities.

Results

The geometric features of the Ultimate Pit Limits (H_{UPL} and OSA) obtained as the result of each iteration of the design process (Figure 5a) are reported in Table 5. A total of six iterations was performed for the traditional design based on planar pitwalls, whilst for the design based on optimal pitwalls, two iterations were enough to reach convergence.

Table 5 Iterations performed to find the optimal Ultimate Pit Limit

Iteration for planar pitwalls	H_{UPL},i-1 [m]		OSA [deg]		H_{UPL},i [m]	
	S1	S2	S1	S2	S1	S2
1	370	360	44.1	37.1	260	140
2	260	140	49.5	51.7	280	260
3	280	260	48	42.1	280	230
6	280	230	48	43.8	280-270	230
Iterations for optimal pitwalls	H_{UPL},i-1 [m]		OSA [deg]		H_{UPL},i [m]	
	S1	S2	S1	S2	S1	S2
1	270	220	50.5	47.4	280	250
2	280	250	50.1	51.3	280	150

Note that to have a consistent and fair comparison between the two designs we adopted a design procedure envisaging iterations between the geotechnically based design of the pitwall and the pit optimization carried out by Whittle (Figure 5). However, practitioners may perform fewer iterations or not at all due to time constraints accepting a less optimal pit design. Nevertheless in case of no iteration, *i.e.* looking at the results obtained after iteration 1 in Table 5 we can state that the adoption of optimal pitwalls provides financial gains of the same order of magnitude.

Pitwall profiles

The pitwall profiles obtained as result of the pit design process are plotted in Figure 11a for pit sector 1 and Figure 12a for pit sector 2. The Factor of Safety of all the pitwall profiles were verified by performing a LEM analysis with the Morgenstern – Price method, which is a rigorous LEM method where all equations of equilibrium are imposed on all slices [53], in Slide 2

[28] with default settings. Preliminary analyses were carried out to make sure the results are independent of the number of slices adopted and of the domain boundaries chosen. The pitwall profiles employed in the Slide 2 analyses are reported in Figure 11b and 12b for the pit design adopting planar profiles and in Figure 11c and 12c for the pit design adopting optimal profiles together with their FoS. In all the cases the FoS found is less than 1% from the target value of 1.3 (Table 4).For the optimal pitwall profiles given the importance of an independent verification of their FoS, we performed additional stability analyses by an explicit Finite Difference Method with Shear Strength Reduction technique (FDMSSR) employing FLAC3D 7.0 [54] having assigned a unit length in the out of plane direction. In the FLAC analyses, the G-H-B criterion was employed together with the "model factor-of-safety" command and default values for the settings affecting the convergence criterion (specified in terms of unbalanced nodal forces) and the detection of slope failure. Details of the algorithm employed by FLAC to calculate the FoS are provided in the FLAC manual [54]: in summary the standard procedure adopted by FDMSSR as in case of M-C geomaterials [55] is followed with the G-H-B criterion approximated locally by the M-C criterion, $\tau_{max} = tan\Phi_{loc} + c_{loc}$, where local cohesion, c_{loc}, and angle of shearing resistance, $tan\Phi_{loc}$, are calculated from the local value of the minor principal stress and G-H-B parameters. In each FLAC analysis c_{loc} and $tan\Phi_{loc}$ are decreased by dividing them by an increasing reduction factor until active slope failure is detected. The FoS is found as the reduction factor at the verge of slope collapse. Both associated and non-associated with zero dilation analyses were run obtaining practically identical FoS values. The negligible influence of dilatancy on slope stability is good news since its value is not known for the rock types of this mine. The critical failure mechanisms identified by Slide2 and FLAC3D and the associated FoSs are reported in Figure 11c and 12c. In both mine sectors, the FoSs found are less than 1% from the target value of 1.30. Note that FDMSSR is an entirely different method of slope stability analysis from LEM and from LA (which is employed by OptimalSlope) so the fact that the FoSs found by Slide2 and FLAC3D are so close to the ones determined by OptimalSlope gives confidence to geotechnical practitioners about the trustworthiness of the FoS of the pitwall profiles determined by OptimalSlope. In conclusion, the FoS values of the pitwall profiles found by OptimalSlope were independently verified by two most popular geotechnical software employed for the geotechnical verification of open pit mines, Slide2 and FLAC, confirming that the pitwall profiles determined by OptimalSlope are as safe as their planar counterparts.

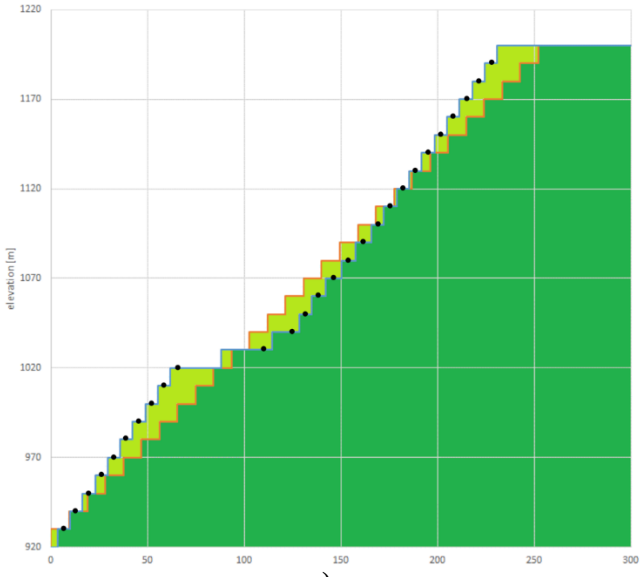

a)

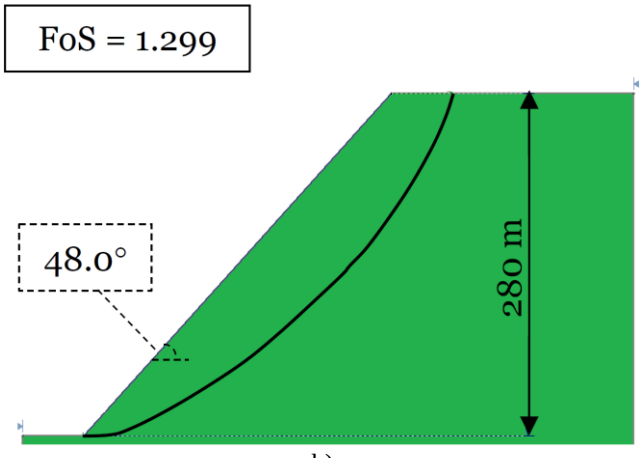

b)

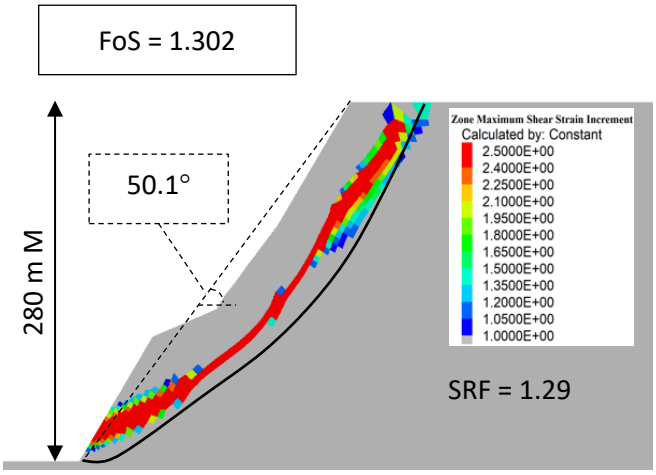

c)

Figure 11 UPL pitwalls for sector S1: a) comparison between the pitwall profile for traditional design (planar pitwall is in orange) and the optimal design (optimal pitwall is in blue, the black dots represent the x_i, z_i coordinates obtained as output from OptimalSlope); b) failure mechanism (black line) and Factor of Safety determined by 2D Limit Equilibrium Method (Slide2) for the planar profile; c) failure mechanism (black line) and Factor of Safety determined by 2D Limit Equilibrium Method (Slide2) and shear strain magnitude determined by Finite Difference Method with Shear Strength Reduction (FLAC3D) for the optimal profile (the black dots represent the x_i, z_i coordinates obtained as output from OptimalSlope).

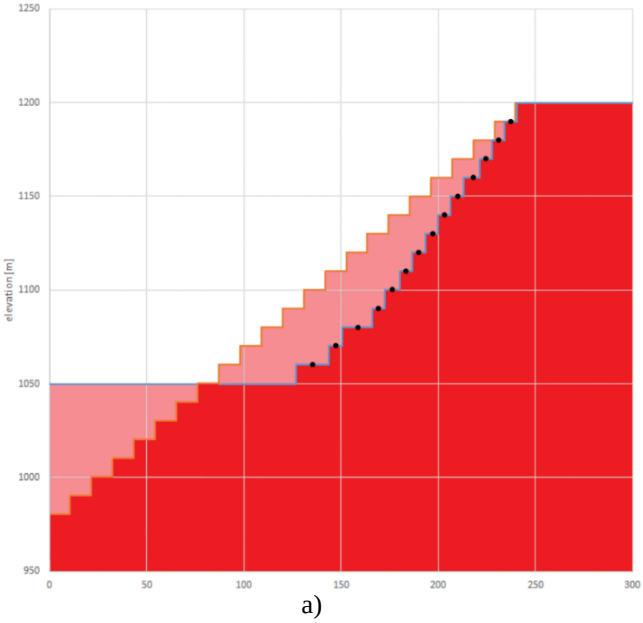

a)

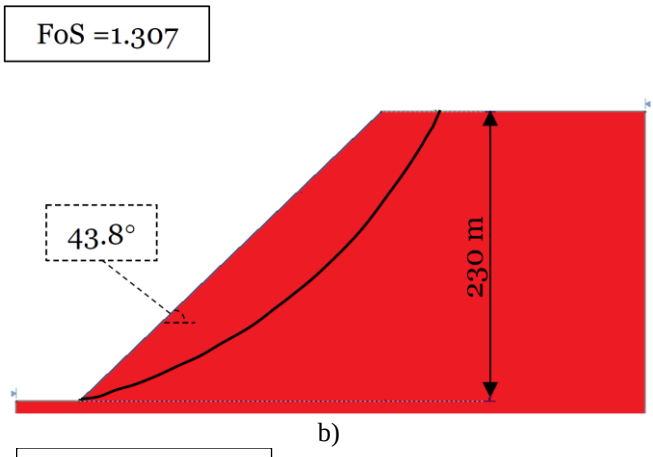

b)

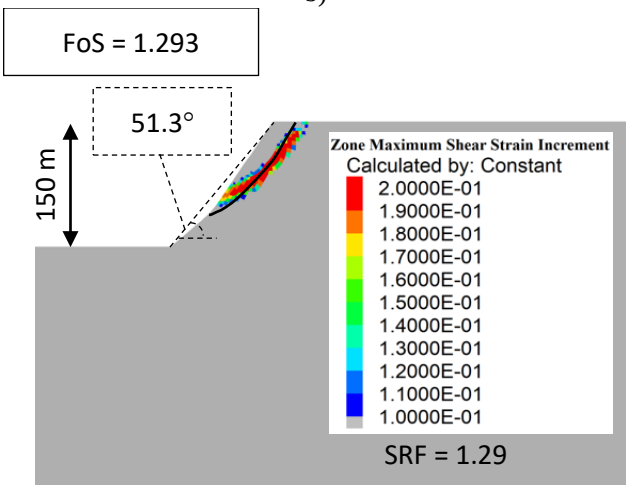

c)

Figure 12 UPL pitwalls for sector S2: a) comparison between the pitwall profile for traditional design (planar pitwall is in orange) and the optimal design (optimal pitwall is in blue, the black dots represent the xi, zi coordinates obtained as output from OptimalSlope); b) failure mechanism (black line) and Factor of Safety determined by 2D Limit Equilibrium Method (Slide2) for the planar profile; c) failure mechanism (black line) and Factor of Safety determined by 2D Limit Equilibrium Method (Slide2) and shear strain magnitude determined by Finite Difference Method with Shear Strength Reduction (FLAC3D) for the optimal profile (the black dots represent the xi, zi coordinates obtained as output from OptimalSlope).

Figures 11a and 12a allow a visual comparison between the planar pitwall profile of a traditional design, demarcated by the orange line, and the optimal pitwall profile, demarcated by the blue line. Considering pit sector S1, the overall height of the profiles is the same. The optimal profile is clearly steeper than the planar one. The area coloured in light green (Figure 11a) highlights the difference between the two profiles: apart from the small difference in the central zone, the optimal profile

requires significantly less rock excavation (see the bottom and top third parts). Considering now pit sector S2, the overall heights of the profiles are significantly different with the optimal one being 70 m less deep than the planar one (Figure 12a). Once again the optimal profile is steeper than the planar one. Comparing the two profiles, the volumes of rock excavated look similar albeit distributed differently in space. In the upper half of the pitwall, the optimal profile requires a larger excavation to extract mainly ore whereas the planar profile requires extraction of ore to a deeper depth.

3D slope stability analysis

In Fig13a and 13b are plotted the 3D views of the Ultimate Pit Limits obtained for the traditional design based on planar pitwalls and for the design based on optimal pitwalls respectively. It is apparent that in both cases a multi-pit shell made by roughly two conical shapes, one distinctly deeper than the other one, is obtained. This is due to the different rock properties and orebody distributions between sector S1 and S2 with each cone lying within a pit sector.

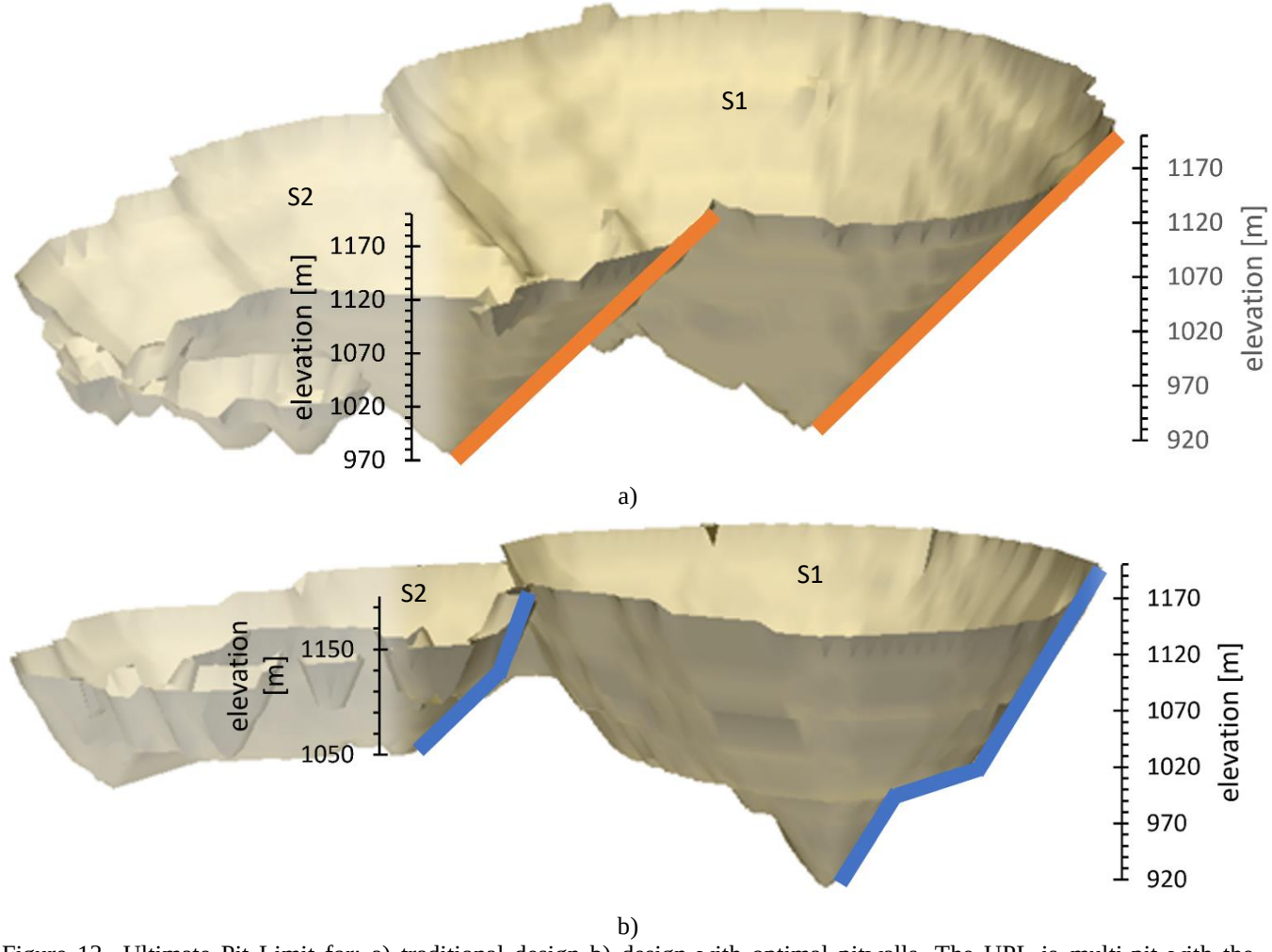

Figure 13 Ultimate Pit Limit for: a) traditional design b) design with optimal pitwalls. The UPL is multi-pit with the boundary between two conical shells roughly corresponding to the boundary between pit sector S1 and S2.

The FoS of the entire UPL was verified by performing a 3D FDM analysis with FLAC3D 7.0 [44]. Note that the numerical settings adopted in the 3D stability analysis were the same as those employed for the 2D analyses reported in section "Pitwall profiles" for sake of consistency. The critical failure mechanism identified by the software and the FoS contour maps are plotted in Fig 14. To check for any potential effect of mesh dependency two analyses were run: one for a coarser (but still fine) mesh and another one for a finer mesh obtained by halving the element sizes of the first mesh. Throughout the entire mine, the minimum FoS

found was 1.70 for the first analysis and 1.67 for the second analysis: such a small difference implies the mesh size adopted is sufficiently small so that the resulting FoS is not affected by mesh size for practical purposes. We can then assume convergence of the FoS from the FLAC3D analysis to 1.67. which is significantly higher than the FoS values obtained by the 2D FLAC analyses of Section 4.1, of ~1.30 and ~1.31 respectively. The main reason for this is due to arching effects that in case of slope shapes concave in plan view enhance stability [56,6]. In this case the very pronounced planar concavity of the UPL acts to constrain movement. This is not taken into account by 2D analyses, that as a consequence are conservative.

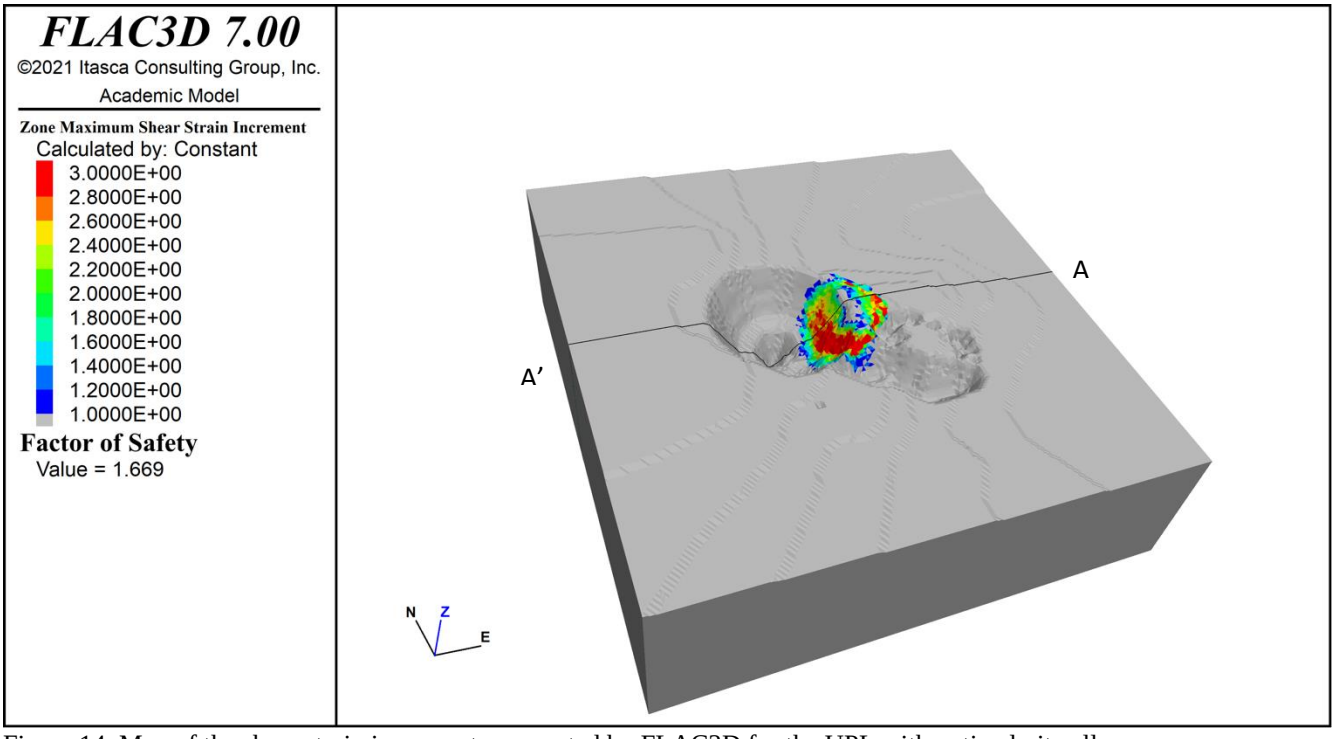

Figure 14 Map of the shear strain increments computed by FLAC3D for the UPL with optimal pitwalls.

Key financial indicators

In Table 6 the key output data for the two design cases are provided. The net present value (NPV) for the design based on optimal pitwalls is around 12 million USD higher than the NPV of the design based on planar pitwalls. Therefore adoption of the optimal profiles would lead to an increase of NPV of 34%. Such an increase is to be ascribed to a very substantial decrease of rockwaste volume, around 15%, from 23.7·106 tonnes to 20.7·106 tonnes, whilst the amount of ore extracted is similar. This implies a reduction of the Stripping Ratio from 0.40 to 0.35. Another metric measuring the financial return of a mine is the Internal Rate of Return (IRR). Adoption of the optimal profiles leads to an IRR of 15.8% instead of the 13.9% obtained from the design with planar pitwalls. Since an IRR of 15% is considered by some companies as a threshold for the viability of a mining project, it can be said that for this mine the adoption of optimal pitwalls could make the difference in terms of the economic viability of the mine project.

Table 6 Pit optimisation economic and metallurgical results

UPL output	Planar pitwalls		Optimal pitwalls	
	S1	S2	S1	S2
Overall Slope Angle [deg]	48	43.8	50.1	51.3
H_{UPL} [m]	270	220	280	150
Waste [t]	23,707,500		20,651,462	
Ore [t]	59,314,446		59,232,285	
Stripping Ratio [-]	0.40		0.35	
NPV [USD]	34,561,747		46,231,284	
IRR [%]	13.9		15.8	
Life [year]	12.22		12.12	
Payback [year]	3.89		3.57	
NPV increase [%]	33.8			

Production schedules

In Figure 15 the pit-by-pit graph of the mine is plotted for both the traditional design based on planar pitwalls (Fig 15a) and the design based on optimal pitwalls (Fig 15b). The vertical black lines indicate the pitshells selected as pushbacks including the UPL (line most to the right). In both cases the UPL has been

selected as the pushback corresponding to the peak of the discounted specified case scenario curve (green curve). The fact that the specified case scenario curves exhibit a plateau implies the choice provides a robust NPV optimum. In Figure 16 the amount of tonnage is plotted against the life of the mine in years. It can be seen that an almost uniform amount of ore is to be extracted year after year for both designs. A constant production over time is a highly desirable feature from a logistical point of view.

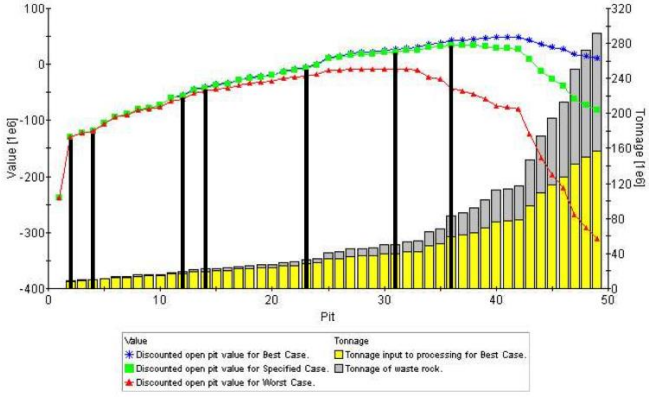

a)

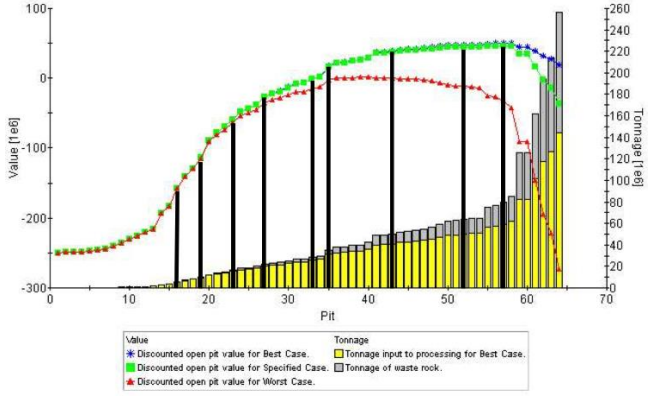

b)

Figure 15 Pit-by-pit graph showing Net Present Value in USD (left vertical axis) and tonnage of mined ore and wasterock (right vertical axis) plotted against nested pitshell number. Each pitshell corresponds to a different revenue factor (fixed intervals were used): a) traditional mine design b) design based on optimal pitwall profiles. The vertical black lines indicate the pitshell selected as pushbacks including the Ultimate Pit Limit (line most to the right).

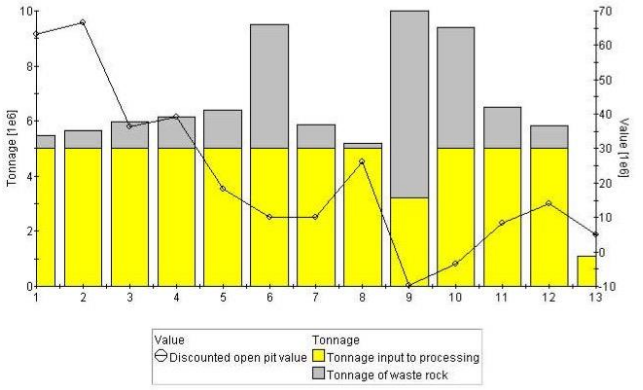

a)

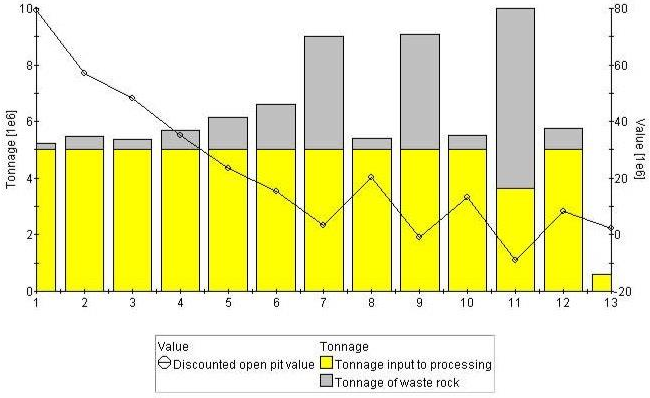

b)

Figure 16 Ore (yellow) and rock waste (grey) tonnage (left vertical axis) and cashflows in USD (right vertical axis) plotted against time in years for: a) traditional mine design b) design based on optimal pitwall profiles.

Environmental indicators

Recently several methods have been proposed in the literature to calculate the Life Cycle Assessment for open pit mines. Here, we have computed the energy requested to mine both orebody and waste rock together with the associated carbon footprint for both design types (design with planar pitwalls and with optimal pitwalls) based on [57]. In the Appendix all the equations employed for these calculations are provided. Note that energy consumption and carbon footprint are calculated for each mined block of the UPLs with block properties such as grade, mass and distance to a reference point on the surface used to estimate the energy requirement to produce 1 tonne of mined ore. The energy requirement per tonne is then translated into carbon footprint by using characterization factors and includes scope 1, 2 and 3 emissions associated with drilling, blasting, extraction, loading and hauling [58]. This approach has been employed in [59] to incorporate sustainability parameters directly into the ore body block model, and include them into strategic pit optimization. The

characterization factors were taken from [60] having assumed the electricity production mix for Chile where the mine is located. The results are provided in Table 7 below.

Table 7 Energy consumption and carbon footprint for the two design options considered

	Design based on Planar pitwalls	Design based on Optimal pitwalls	Difference between options: Optimal – Planar	Difference between options: Optimal – Planar (%)
Energy [MJ]	2.134×10^9	2.052×10^9	-8.25×10^7	-3.9%
Carbon footprint [Mt CO_2 eq]	4.458	4.289	-0.167	-3.8%

It emerges that the adoption of optimal pitwalls leads to reductions of carbon footprint and energy consumption of 0.17 million tonnes CO2 eq and 82.5 million MJ respectively over the life of the mine. To provide some context a reduction of 0.17 million tonnes CO2 eq is equivalent to the carbon sequestered by 2.8 million tree seedlings grown for 10 years and to the greenhouse gas emissions avoided by 35 wind turbines producing electricity for a year [61]. Both carbon footprint and energy usage savings are achieved by a significant reduction of rockwaste excavation, around 15% in volume, with the amount of orebody extracted being very similar in the two design options considered (see Table 6).

Conclusions

It is well known that the steepness of the pitwalls of an open pit mine bears a large influence on the volume of rockwaste to be extracted so that any increase of steepness leads to a better stripping ratio and therefore higher profitability and carbon footprint and energy use reductions. In current design practices mines tend to be designed on the basis of planar pitwalls, i.e. with a constant inter-ramp angle (IRA) or even overall slope angle (OSA), in each sector of the mine. However looking at the final geometry of any pit cross-section, this is anything but planar due to the need to accommodate for benches, step-outs and roads, therefore the assumption of constant IRA and/or OSA adopted at the design stage is a simplification which can and should be removed if a better design can be achieved as result. It seems only natural to wonder whether pitwalls of non-linear shape could be used instead of planar ones. In the geotechnical literature some specific shapes of non-linear profiles have already been proven to be more stable than the planar one ([8], [9], [10] and [11]) for uniform c-f slopes. The code OptimalSlope [12] determines optimal shapes for both uniform and non-uniform slopes with any number of rock layers, and for geomaterials whose strength is described by either the Mohr-Coulomb criterion or the generalized Hoek-Brown criterion. In this paper we employed the geotechnically optimal pitwall profiles determined by OptimalSlope to systematically maximize the OSA of the pitwalls of a soon to be opened copper mine . The long-term schedule of the mine was carried out using Geovia Whittle first employing planar pitwalls, secondly adopting the optimal pitwall profiles determined by OptimalSlope.

The adoption of geotechnically optimal profiles led to a 34% higher net present value and very significant reductions of carbon footprint and energy consumption, 0.17 million tonnes CO2 eq and 82.5 million MJ respectively, due to a 15% reduction of waste rock volume in comparison with the traditional design based on planar pitwalls. The stability of all the pitwall cross-sections determined by OptimalSlope was independently checked by two most popular geotechnical software packages, namely Rocscience Slide2 to perform Limit Equilibrium Method analyses with the Morgenstern-Price method and FLAC3D to perform Finite Difference Method analyses with Shear Strength Reduction. The Factor of Safety values determined by Slide2 and FLAC turned out to be in very close agreement (less than 1% difference) to the ones determined by OptimalSlope. Finally a 3D stability analysis for the entire ultimate pit was carried out by FLAC3D verifying the resulting FoS was well above the specified acceptability criterion (FoS=1.3 in this case) across the entire pit. Also we have employed OptimalSlope in the design of other two case studies, both gold mines: a contemporary mine being developed by Kinross [64] and the well known case of the McLaughlin mine where a publically available block model was employed [65]. In [64] OptimalSlope was employed in a more complex geological context with several rock formations of different M–C strength which required the design of five different pit sectors and a significant overburden which required the inclusion of uniform surcharges to be applied on the upper topography of the pit walls. In both cases, employing optimal pitwall profiles in the mine design led to significant increases of NPV, up

to 52.7%, and substantial decreases of energy consumption and carbon footprint, both a result of the decrease in mine stripping ratios due to the adoption of geotechnically optimal profiles.

The case study considered here is of a relatively small pit in a medium-strong rock. It can be expected that the increase of pitwall inclination will be more significant in weaker rocks. Also, we know that the larger the depth of a pit, the more significant the impact of the pitwall steepness is on the economics of the mine. Therefore, we believe the financial and environmental gains obtained for large and deep pits can be even higher. Finally, irrespective of the size of the open pit mine, because a planar slope is a particular case of a curved one obtained by setting the radius of curvature to infinity along the entire slope, there is a theoretical argument to suggest that adopting planar pitwall profiles is a suboptimal choice for most rock masses and soil types apart from the case of frictional (zero cohesion) soils.

Availability of data and material: the block model is subject to an NDA from the mining company. The corresponding author can redirect any request to the mining company.

Code availability: the input and outputs files of OptimalSlope, Whittle and Slide 2 can be made available upon request to the corresponding author.

Authors' contributions S. Utili: ideation and conceptualization of the work, methodology, result analysis, writing of the paper. **A. Agosti:** productions of the results by running OptimalSlope and the pit optimiser software packages, methodology, result analysis, production of figures and tables. **N. Morales:** result analysis, reviewing and editing. **C. Valderrama**: performance of the FLAC analyses **R. Pell:** section "Environmental indicators" result analysis, reviewing and editing. **G. Albornoz:** reviewing and editing.

Appendix

The appendix presents the formulae employed to compute the energy consumption and the carbon footprint associated with drilling, blasting, loading, and hauling for all the Ultimate Pit Limit blocks.

Our calculations were based on the formulae provided by , who were the first to provide a comprehensive set of equations for the calculation of energy consumption and GWP emissions for blocks of a block model. First the energy consumption of each block is evaluated based on the processes affecting it and then its GHP is derived from the calculated energy consumption. Muñoz et al. [57] identify three main stages of energy consumption, namely mining, concentrating and hydrometallurgical. The concentrating and hydrometallurgical stages have not been considered since we do not know the passing material at the feed nor at the product of the crusher. Also no information about the processing method is available. However, because the amount of orebody extracted for processing for the traditional pitwall design and design by optimal pitwalls almost identical (see table 6), we do not expect them to alter the differences in terms of carbon footprint and energy consumption between the two designs considered in the paper. The energy consumption due to mining, E_M, is made of four components [57]:

$$E_M = E_{drilling} + E_{blasting} + E_{loading} + E_{hauling}$$

with $E_{drilling}$ the energy consumption due to drilling, $E_{blasting}$ due to blasting, $E_{loading}$ due to loading of the mined material on dumper trucks and $E_{hauling}$ due to hauling to either processing plant or dump.

For drilling, the energy consumption is calculated as [57] :

$$E_{drilling}[MJ/t] = \frac{A \cdot E_V \cdot L \cdot N}{\eta_{drill} \cdot m_b}$$

where:

$A = 116.9\ \mathrm{cm}^2$ is the area of the drill hole;

$L = 35\ cm$ is the charged length of the drill hole;

$N = 10$ is the number of drill holes for each block;

$E_{\mathrm{v}} = 112 - 148\ \mathrm{J}/cm^3$ is the drilling specific energy which depends on the rock type and was estimated based on a unified classification system of rocks according to their drillability [62];

$\eta_{drill} = 80\%$ is the assumed driller efficiency;

m_b is the mass of the block in ton.

The specific energy that an explosive can deliver when detonated is computed with the formula [57]:

$$E_{blasting}[MJ/t] = LF \cdot E_{expl}$$

where:

$LF = 6\ \mathrm{kg}_{expl}/\mathrm{t}$ is the load factor, defined as the amount of explosive per ton of detonated rock;

$E_{expl} = 3.81581\ \mathrm{MJ/kg}_{expl}$ is the specific explosive energy [57] for ANFO, the type of explosive here employed.

The specific energy that a front loader consumes to load up the fractured material on the dumper can be computed with the expression:

$$E_{loading}[MJ/t] = \frac{P_L \cdot T}{\eta_{loader} \cdot m_{truck}}$$

where:

$P_L = 0.18\,MW$ is the front loader power (having assumed a CAT 950 GC);

T=45 s is the assumed average time to meet the loading capacity of the dumper using the front loader;

$\eta_{load} = 70\%$ is the assumed front loader efficiency;

$m_{truck} = 92.2\,t$ is the loading capacity of the dumper (having assumed a Komatsu HD 785-8), assuming the dumper fully loading at every trip.

The specific energy to haul a ton of material from the pit to the processing plant or the waste dump can be computed with the formula [57]:

$$E_{hauling}[MJ/t] = \frac{9.81 \cdot \mathrm{S} \cdot \left(m_{\mathrm{truck}} \cdot i + (\mathrm{R_s} + \mathrm{R_i}) \cdot (2 \cdot \mathrm{M_{truck}} - m_{\mathrm{truck}})\right)}{m_{\mathrm{truck}}}$$

where:

S is the distance of the i-th block from the processing plant or waste dump in km which we have calculated for each block;

$i = 10\,\%$ is the inclination of the ramp;

$\mathrm{R_s} = 2\,\%$ is the rolling resistance of the surface from [63];

$\mathrm{R_i} = 1\%$ is the assumed internal resistance of the dumper;

$\mathrm{M_{truck}} = 166\,t$ is the total mass of the loaded dumper (Komatsu HD 785-8).

To calculate the carbon footprint, the specific energy consumptions per tonne are translated into specific carbon footprint using characterization factors to include scope 1, 2 and 3 emissions associated with the mining activities by using the following equation [57]:

$$GWP\left[\frac{t_{CO_{2,eq}}}{t}\right] = \alpha \cdot \frac{E_{drill} + E_{load} + E_{haul}}{1000} + \beta \cdot \frac{E_{drill} + E_{load} + E_{haul}}{1000} + \delta \cdot \frac{E_{blast}}{1000}$$

where the coefficients α, β, δ are the coefficient of carbonization for diesel, electrical power matrix, and explosive taken from the Ecoinvent database [60]. Their values are:

α=0.09159 $t_{CO_{2,eq}}$/MJ;

β=0.5200 $t_{CO_{2,eq}}$/MJ;

δ=2.270 $t_{CO_{2,eq}}$/MJ .

Finally, the total carbon dioxide emissions are computed as the multiplication of the specific carbon footprint by the tonnages of the Ultimate Pit Limit.

References

1. Randolph M (2011) Current trends in mining. In: Darling P (ed) SME Mining Engineering Handbook. 3rd edn. Society for Mining Metallurgy and Exploration, pp 11-19
2. Hustrulid W, Kutcha M, Martin R (2013) Open pit mine planning and design. CRC Press
3. Brown ET (2004) Geomechanics: The critical engineering discipline for mass mining. In: Karzulovic A, Alfaro M (eds) Massmin 2004, Santiago, Chile, 2004. Chilean Engineering Institute, Santiago, Chile
4. Martin D, Stacey P (2018) Guidelines for Open Pit Slope Design in Weak Rocks. CSIRO Publishing
5. Newman J (1890) Earthwork Slips and Subsidences Upon Public Works: Their Causes, Prevention, and Reparation. Spoon, London
6. Hoek E, Bray J (1977) Rock Slope Engineering. second edn. The Institution of Mining and Metallurgy, London
7. Rana MH, Bullock WD (1969) The design of open pit mine slopes. Canadian Mining Journal 58-66
8. Utili S, Nova R (2007) On the optimal profile of a slope. Soils and Foundations 47:717-729
9. Jeldes A, Drumm EC, Yolder DC (2015) Design of Stable Concave Slopes for Reduced Sediment Delivery. ASCE Journal of Geotechnical and Geoenvironmental Engineering 142
10. Vahedifard F, Shahrokhabadi S, Leshchinsky D (2016) Optimal Profile for Concave Slopes under Static and Seismic Conditions. Canadian Geotechnical Journal 53 (9):1522– 1532
11. Vo T, Russell AR (2017) Stability Charts for Curvilinear Slopes in Unsaturated Soils. Soils and Foundations 57 (4):543–556
12. Utili S (2016) OptimalSlope: Software for the determination of optimal profiles for slopes and pit-walls. Registered at the United States Copyright Office
13. Bendsoe M, Sigmund O (2004) Topology optimisation. 2nd edn. Springer, Berlin. doi:doi.org/10.1063/1.3278595
14. Fin J, Borges LA, Fancello EA (2019) Structural topology optimization under limit analysis. Structural and Multidisciplinary Optimization 59 (4):1355-1370. doi:10.1007/s00158-018-2132-y
15. Chen WF (1975) Limit analysis and soil plasticity. Elsevier, New York
16. Hoek E (1994) Strength of rock and rock masses ISRM News Journal 2 (2):4-16
17. Hoek E, Brown ET (1997) Practical estimates of rock mass strength. International Journal of Rock Mechanics and Mining Sciences 34 (8):1165-1186
18. Read J, Stacey P (2009) Guidelines for Open Pit Slope Design. CSIRO, Australia
19. Hoek E, Brown ET (2019) The Hoek–Brown failure criterion and GSI – 2018 edition. Journal of Rock

Mechanics and Geotechnical Engineering 11 (3):445-463. doi:10.1016/j.jrmge.2018.08.001
20. Renani RH, Martin CD (2020) Slope Stability Analysis using Equivalent Mohr–Coulomb and Hoek–Brown criteria. Rock Mechanics and Rock Engineering 53 (1):13-21. doi:10.1007/s00603-019-01889-3
21. OptimalSlope (2021): Software for the determination of optimal profiles for slopes and pitwalls. User manual. http://optimalslope.com/files/OptimalSlope_V_0_6_User_Manual.pdf.
22. Parra A, Morales N, Vallejos J, Nguyen PMV (2017) Open pit mine planning considering geomechanical fundamentals. International Journal of Mining, Reclamation and Environment 32 (4):221-238. doi:10.1080/17480930.2017.1278579
23. Stewart A, Hawley P, Rose N, Gilmore B (2004) Mining applications. In: Wyllie D, Mah C (eds) Rock slope engineering. 4th Edition edn. Spon press, New York, pp 357-376
24. Lerches H, Grossmann I (1965) Optimum design of open pit mines. *CIM Transactions* 68: 17-24
25. Hochbaum D (2008) The pseudoflow algorithm: a new algorithm for the maximum-flow problem. Oper Res 58 (4):982–1009
26. Khalokakaie R, Dowd P, Fowell R (2000) Lerchs-Grossmann algorithm with variable slope angles. *Trans Inst mining & metallurgy section A* 109: A77-A85
27. Khalokakaie R, Dowd P, Fowell R (2000) Incorporation of slope design into optimal open pit design algorithms. Transaction of the Institute of mining and metallurgy section A 109:A70-A76
28. Rocscience (2021) Slide 2
29. Geovia (2021) Surpac user manual.
30. Geovia (2021) Whittle user manual. 4.7.3 edn.
31. Datamine (2021) Studio OP. 2.8 edn. Datamine
32. Datamine (2021) Studio NPVS. 1.0.51.0 edn.
33. Maptek (2021) Vulcan Open Pit Mine Planning. 2020.1 edn.
34. Hexagon (2021) HxGN MinePlan Engrg OP LTP Pro.
35. Hexagon (2021) HxGN MinePlan Project Evaluator.
36. Kliche CA (2011) Slope stability. In: Darling P (ed) SME Mining Engineering Handbook. 3rd edn. Society for Mining Metallurgy and Exploration, pp 495-525
37. Lorig L, Read J, Stacey P (2009) Slope design methods. In: Read J, Stacey P (eds) Guidelines for open pit slope design. CRC Press, pp 237-264
38. Rocscience (2020) SWedge user manual.
39. SRK (2016) Frac_rock: programme for the analysis of discontinuous rock masses.
40. Call RD (1992) Slope stability. In: Hartman HL (ed) SME Mining Engineering Handbook, vol 1. 2nd edn. Society for Mining Metallurgy and Exploration, Littleton, Colorado (USA) Ch 10.4
41. Ryan TM, Pryor PR (2001) Designing catch benches and interramp slopes. In: Hustrulid W, McCarter M, van Zyl D (eds) Slope stability in surface mining. Society for Mining Metallurgy Exploration, pp 27-38
42. Alejano LR, Pons B, Bastante FG, Alonso E, Stockhausen HW (2007) Slope geometry design as a means of controlling rockfalls in quarries. International Journal of Rock Mechanics & Mining Sciences 44: 903-921
43. Rocscience (2002) RocFall user manual.
44. Basson FRP (2012), 'Rigid body dynamics for rock fall trajectory simulation', in Proceedings of the 46th US Rock Mechanics & Geomechanics Symposium 24–27 June 2012, American Rock Mechanics Association, Chicago
45. Bar N, Nicoll S, Pothitos F (2016) Rock fall trajectory field testing, model simulations and considerations for steep slope design in hard rock. First Asia Pacific Slope Stability in Mining (APSSIM) Conference, Brisbane, Australia
46. Gibson W, de Bruyn IA, Walker DJH (2006) Considerations in the optimisation of bench face angle and berm width geometries for open pit mines. Proc. South African Institute of Mining and Metallurgy Int Symp on Stability of rock slopes, Symp series S44 Stability of rock slopes in open pit mining and civil engineering situations, pp 557-579
47. Coetsee S (2020) An overview of bench design for cut slopes with an example of an advanced dataset assessment technique. Proc of the 2020 Int Symp on Slope Stability in Open Pit Mining and Civil Engineering, pp 731-748
48. Tang GP, Zhao LH, Li L, Yang F (2015) Stability charts of slopes under typical conditions developed by upper bound limit analysis. *Comp & Geotechnics*, 65: 233-240.
49. Hoek E, Carranza-Torres C, Corkum B (2002) Hoek-Brown failure criterion 2002 edition. In: Hammah R et al. (eds) Proc 5th North American Rock Mechanics Symp, University of Toronto, Toronto, pp 267-273.
50. Li AJ, Merifield RS, Lyamin AV (2008) Stability charts for rock slopes based on the Hoek-Brown failure criterion. Int. J. Rock Mechanics & Mining Sciences, 45: 689-700.
51. Taylor D (1937) Stability of earth slopes. J Boston Soc of Civil Engineers 24:197-246
52. Taylor D (1948) Fundamentals of soil mechanics. John Wiley and sons, New York
53. Morgenstern N, Price V (1965) The analysis of the stability of general slip surfaces. Geotechnique 15: 79-93
54. Itasca International Inc. (2021) FLAC 3D user manual
55. Dawson E, Roth W, Drescher A (1999) Slope stability analysis by strength reduction. Geotechnique 49: 835-840
56. Lorig L, Varona P (2001) Practical Slope Stability Analysis Using Finite Difference Codes. In: Slope Stability in Surface Mining, Colorado, 2001. Society for Mining, Metallurgy and Exploration, pp 115–124
57. Munoz J., Guzman RR., Botin JA. (2014). Development of a methodology that integrates environmental and social attributes in the ore resource evaluation and mine planning. Int J Mining & Mineral Engineering 5:38-58. doi:10.1504/IJMME.2014.058918
58. Greenhouse Gas Protocol (2019) https://ghgprotocol.org/. Accessed 21/03/2021
59. Pell R, Tijsseling L, Palmer LW, Glass HJ, Yan X, Wall F, Zeng X, Li J (2019) Environmental optimisation of mine scheduling through life cycle assessment integration. Resources, Conservation and Recycling 142:267-276. doi:10.1016/j.resconrec.2018.11.022
60. Wernet G, Bauer C, Steubing B, Reinhard J, Moreno-Ruiz E, Weidema B (2016) The ecoinvent database version 3 (part I): overview and methodology. The International Journal of Life Cycle Assessment 21

(9):1218-1230. doi:10.1007/s11367-016-1087-8
61. Greenhouse gas equivalencies calculator (2021) https://www.epa.gov/energy/greenhouse-gas-equivalencies-calculator. Accessed 21/03/2021
62. Isheyskiy, V., Sanchidrián, J.A., (2020). Prospects of Applying MWD Technology for Quality Management of Drilling and Blasting Operations at Mining Enterprises. Minerals 10, 925.
63. Soofastaei, A., Aminossadati, S.M., Arefi, M.M., Kizil, M.S., 2016. Development of a multi-layer perceptron artificial neural network model to determine haul trucks energy consumption. *Int J of Mining Sci & Technology* 26, 285–293.
64. Agosti, A., Utili S., Gregory D., Lapworth A., Samardzic J., Prawasono A. (2021) Design of an open pit goldmine by optimal pitwall profiles. *CIM Journal*, 12(4): 149-168.
65. Agosti, A., Utili S., Valderrama, C., Albornoz, G. (2021) Optimal pitwall profiles to maximise the Overall Slope Angle of open pit mines: the McLaughlin mine. ACG *Proceedings of Slope stability in mining conference*, 69- 82, Perth (Australia). doi:10.36487/ACG_repo/2135_01